Direct Power Compensation in AC Distribution Networks with SCES Systems via PI-PBC Approach

Walter Gil-González [1,*] [ID], **Federico Martin Serra** [2] [ID], **Oscar Danilo Montoya** [1,3] [ID], **Carlos Alberto Ramírez** [4] **and César Orozco-Henao** [5] [ID]

[1] Laboratorio Inteligente de Energía, Universidad Tecnológica de Bolívar, km 1 vía Turbaco, Cartagena 131001, Colombia; omontoya@utb.edu.co
[2] Laboratorio de Control Automático (LCA), Universidad Nacional de San Luis, Villa Mercedes 5730, Argentina; fmserra@unsl.edu.ar
[3] Facultad de Ingeniería, Universidad Distrital Francisco José de Caldas, Carrera 7 No. 40B - 53, Bogotá D.C 11021, Colombia
[4] Facultad de Ciencias Básicas, Universidad Tecnológica de Pereira. AA: 97, Pereira 660003, Colombia; caramirez@utp.edu.co
[5] Electrical and Electronic Engineering Department, Universidad del Norte, Barranquilla 080001, Colombia; chenaoa@uninorte.edu.co
* Correspondence: wjgil@utp.edu.co

Abstract: Here, we explore the possibility of employing proportional-integral passivity-based control (PI-PBC) to support active and reactive power in alternating current (AC) distribution networks by using a supercapacitor energy storage system. A direct power control approach is proposed by taking advantage of the Park's reference frame transform direct and quadrature currents (i_d and i_q) into active and reactive powers (p and q). Based on the open-loop Hamiltonian model of the system, we propose a closed-loop PI-PBC controller that takes advantage of Lyapunov's stability to design a global tracking controller. Numerical simulations in MATLAB/Simulink demonstrate the efficiency and robustness of the proposed controller, especially for parametric uncertainties.

Keywords: distribution networks; direct power control; global tracking controller; passivity-based control; supercapacitor energy storage system

1. Introduction

Supercapacitors are promising energy storage technologies with high energy density and high charging/discharging capabilities [1]. They allow for the storage of electrical energy in electric fields, increasing their efficiency in comparison with mechanical or chemical devices [2]. Supercapacitor energy storage (SCES) and superconducting magnetic energy storage (SMES) are the only two devices that store energy in the form of electromagnetic fields [3]. Nevertheless, SCES systems are preferred because they work with voltage source converters [1], which are common and represent the cheapest option when compared with the current source converters in SMES applications [4]. Additionally, another advantage of using SCES over SMES systems is that the former does not require special thermal covers, such as those needed for cooling systems based on liquid hydrogen, helium, or nitrogen [3]. This increases the acquisition, installation, and maintenance of SMES systems.

The integration of SCES systems via voltage source converters allows controlling the active and reactive power independently by formulating a dynamic model in any reference frame (i.e., time domain or *abc*, Clark's or $\alpha\beta$, and Park's or *dq* reference frames, respectively) [5]. In addition, the dynamical model of the SCES system exhibits a nonlinear structure that makes it necessary to propose nonlinear controllers to deal with its operational goals. Multiple controllers for SCES

systems integration in electrical networks have been proposed such as feedback linearization methods [6], interconnection and damping PBC approaches [3,5], linear matrix inequalities [7], classical proportional-integral controls [8], adaptive predictive control [9], or proportional-integral passivity-based control (PI-PBC) methods [2], that typically control active and reactive power in an indirect form by controlling the currents on the AC side of the converter. Two interesting approaches based on IDA-PBC and PI-PBC approaches have been reported by [10,11] to control SMES and SCES systems in autonomous applications of single-phase microgrids; these PBC approaches take the advantages of the port-Hamiltonian modeling to propose asymptotically stable controllers of Lyapunov. Authors confirm that single-phase converters allow the control of active and reactive power independently; nevertheless, the main disadvantage is the dependence on the parameters of the control laws, which complicates their application over systems with parametric uncertainties.

Note that PBC approaches are preferred to operate SCES systems because their dynamic models exhibit a port-Hamiltonian (pH) structure in open-loop, which is a suitable structure that is employed in PBC designs. Because it allows proposing closed-loop control structures that can guarantee stable operation in the sense of Lyapunov [12]. Even though the PI-PBC method has been previously presented for SCES systems by [2], who presented a direct power control structure, we proposed a robust parametric approach that avoids prior knowledge on the system parameters (inductance, resistance, and supercapacitor values) and does not require the solution of additional differential equations. This is a gap that is yet to be solved in specialized literature for SCES applications in AC distribution networks. In addition, the main advantage of using direct power control is that the state variables to design the controller are directly active and reactive power. Making more suitable the assignation of the references to control these variables in generation or load compensation applications, while classical approaches work with currents as state variables requiring additional steps regarding active and reactive power control.

The remainder of this paper is organized as follows: Section 2 presents a complete dynamical formulation of the SCES system interconnected to AC grids with a series resistive-inductive filter. In addition, we present its pH intrinsic formulation and its transformation from the current structure to the power ones. Section 3 presents the structure of the proposed PI-PBC approach, highlighting its independence regarding the filter parameters and provides a general proof to guarantee asymptotic convergence. Section 4 reports the general control structure as a function of active and reactive power measures as well as the physical constraints related to the integration of SCES in distribution networks. Section 5 presents the test system, simulating conditions, and numerical results with their corresponding analysis and discussion. Section 6 details the main conclusions derived from this research.

2. Dynamical Modeling

To obtain the dynamical representation of the SCES system integrated with VSC, only Kirchhoff's laws and the first Tellegen's theorem is required. Here, we suppose that all the variables were transformed from the *abc* reference frame into Park's reference frame [5].

$$l\frac{d}{dt}i_d = -ri_d + \omega li_q + v_{sc}u_d - v_d, \tag{1}$$

$$l\frac{d}{dt}i_q = -ri_q - \omega li_d + v_{sc}u_q - v_q, \tag{2}$$

$$c_{sc}\frac{d}{dt}v_{sc} = -i_d u_d - i_q u_q, \tag{3}$$

where l and r are the series inductance and resistance of the AC filter (transformer), respectively; c_{sc} is the capacitance value of the SCES system; i_d and i_q represent the direct- and quadrature-axis currents, respectively, while v_d and v_q are their corresponding voltages; v_{sc} is the voltage in the terminals of the supercapacitor and, u_d and u_q are the modulation indexes of the converter that work as control

inputs. Note that dynamical Model (1)–(3) is a sub-actuate control system because there are $m = 2$ control variables and $n = 3$ states.

Remark 1. *The dynamical Model (1)–(3) exhibits a non-affine port-Hamiltonian structure as follows:*

$$\mathcal{D}\dot{x} = [\mathcal{J}(u) - \mathcal{R}]x + \zeta, \tag{4}$$

where $\mathcal{D} \in \mathbb{R}^{n \times n}$ is the inertia matrix, which is diagonal and positive definite, $\mathcal{J} \in \mathbb{R}^{n \times n}$ and $\mathcal{R} \in \mathbb{R}^{n \times n}$ are the interconnection and damping matrices, such that $\mathcal{J}$ is skew-symmetric and $\mathcal{R}$ is diagonal and positive semidefinite; $x \in \mathcal{R}^n$ and $u \in \mathcal{R}^m$ are the state and control vectors; and $\zeta \in \mathcal{R}^n$ corresponds to the external input vector.

Lemma 1. *The dynamical Model (1)–(3) can be transformed into a direct-power control (DPC) model preserving its non-affine port-Hamiltonian structure by defining the following variables as recommended in [2]: $p = v_d i_d$, $q = -v_d i_q$, and $v = v_d v_{sc}$, where $v_q = 0$ because the PLL is referred to the direct-axis.*

Proof. To obtain a DPC model, let us suppose that the v_d and v_q signals are obtained by implementing a phase-looked loop (PLL), such that they (i.e., v_d and v_q) are constants and well known. Now, if we derive the active and reactive power components, then,

$$\frac{d}{dt}p = v_d \frac{d}{dt}i_d, \tag{5a}$$

$$\frac{d}{dt}q = -v_d \frac{d}{dt}i_q, \tag{5b}$$

where, if we substitute Equation (1) and (2) considering that $v = v_d v_{sc}$, the following result is obtained

$$l\frac{d}{dt}p = -rp - \omega lq + vu_d - v_d^2, \tag{6a}$$

$$l\frac{d}{dt}q = -rq + \omega lp - vu_q. \tag{6b}$$

Note that if we multiply Equation (3) by v_d and rearrange some terms, then

$$c_{sc}\frac{d}{dt}v = -pu_d + qu_q. \tag{7}$$

Finally, when expressions Equations (5) to (7) are rearranged in the form of Equation (4), the proof is completed with

$$\mathcal{D} = \begin{pmatrix} l & 0 & 0 \\ 0 & l & 0 \\ 0 & 0 & c_{sc} \end{pmatrix}, \mathcal{J}(u) - \mathcal{R} = \begin{pmatrix} -r & -\omega l & u_d \\ \omega l & -r & -u_q \\ -u_d & u_q & 0 \end{pmatrix}$$

$$x = \begin{bmatrix} p & q & v \end{bmatrix}^T, \quad \zeta = \begin{bmatrix} -v_d^2 & 0 & 0 \end{bmatrix}^T.$$

□

Remark 2. *Considering the advantages of the pH formulation exhibited by the DPC controller, an appropriate controller to alleviate the active and reactive power oscillations with the SCES systems is the passivity-based control approach because it takes advantage of the pH model to design an asymptotically stable controller in the sense of Lyapunov.*

3. Passivity-Based Control Design

PBC control is a powerful nonlinear control technique that allows designing stable controllers by taking advantage of pH modeling. The main objective of the PBC is to find a set of control laws that help to preserve the pH structure of the dynamical model in closed-loop to guarantee stability in the sense of Lyapunov, using energetic modeling [12]. There are different approaches based on the PBC theory; the most known approach corresponds to the interconnection and damping assignment (IDA-PBC) because it allows working with linear, nonlinear, and non-affine dynamical systems [13]. Nevertheless, there is also an interesting alternative that includes the well-known advantages of the PI actions in the PBC design, which produces a stable PI-PBC approach that guarantees stability in closed-loop operation; however, this approach is only applicable in nonlinear systems with a bilinear structure such as the case of the dynamical models of the power electronic converters [2]. In the next subsection, we will present the general PI-PBC design for bilinear systems.

3.1. Bilinear Representation

To develop a controller based on the PI-PBC approach, let us make the following definition.

Definition 1. *An admissible equilibrium point ($x^\star$) exists for non-linear dynamical Model (4) if its variables are represented in Park's reference frame (direct- and quadrature-axis), such that*

$$0 = [\mathcal{J}(u^\star) - \mathcal{R}]x^\star + \zeta, \tag{8}$$

for some constant control input $u^\star$.

Considering the definition of the equilibrium point, now we use some auxiliary variables to develop a PI-PBC controller as follows: $\tilde{u} = u - u^\star$ and $\tilde{x} = x - x^\star$, where $\tilde{x}$ and $\tilde{u}$ represent the error of the state variables and control inputs.

Note that if we subtract Equation (8) from (4), the following result is obtained

$$\mathcal{D}\dot{\tilde{x}} = [\mathcal{J}(u)x - \mathcal{J}(u^\star)x^\star] - \mathcal{R}\tilde{x}. \tag{9}$$

To simplify Equation (9), let us define the property related to bilinear systems as follows:

Definition 2. *The matrix product $\mathcal{J}(u)x$ has a bilinear structure if it can be separated as a sum as follows*

$$\mathcal{J}(u)x = \mathcal{J}_0 + \sum_{i=1}^{m} \mathcal{J}_i x u_i, \tag{10}$$

where $\mathcal{J}_0$ and $\mathcal{J}_i$ are constant matrices with skew-symmetric structure.

Now, if we consider the Definition 2 in Equation (9) and make some algebraic manipulations, then the below result is obtained:

$$\mathcal{D}\dot{\tilde{x}} = [\mathcal{J}_0 - \mathcal{R}]\tilde{x} + \sum_{i=1}^{m} \mathcal{J}_i \tilde{x} u_i + \sum_{i=1}^{m} \mathcal{J}_i x^\star \tilde{u}_i. \tag{11}$$

Remark 3. *Expression (11) is the essential structure to design PI-PBC controllers for bilinear systems, as demonstrated in [14].*

3.2. Lyapunov's Requirements for Stability Analysis

To guarantee that the dynamical System (11) is stable in the sense of Lyapunov for the equilibrium point $\tilde{x} = 0$, i.e., $x = x^\star$, let us define a candidate Lyapunov function $\mathcal{V}(\tilde{x})$ with hyperboloid structure as presented below

$$\mathcal{V}(\tilde{x}) = \frac{1}{2} \tilde{x}^T \mathcal{D} \tilde{x}. \tag{12}$$

Observe that $\mathcal{V}(\tilde{x})$ meets the first two conditions of the Lyaponov's stability theorem, i.e., $\mathcal{V}(0) = 0$, and $\mathcal{V}(\tilde{x}) > 0$, $\forall \tilde{x} \neq 0$. In addition, if we take the temporal derivative of Equation (12) and substitute Equation (11), the following result is obtained:

$$\dot{\mathcal{V}}(\tilde{x}) = \tilde{x}^T \mathcal{D} \dot{\tilde{x}} = -\tilde{x}^T \mathcal{R} \tilde{x} + \sum_{i=1}^{m} \tilde{x}^T \mathcal{J}_i x^\star \tilde{u}_i, \tag{13}$$

which implies guarantee in stability, if the second term on the right hand side of Equation (13) is negative definite or at least negative semidefinite. To simplify this expression, let us use the input–output relation $\tilde{u} \rightarrow \tilde{y}$ being $\tilde{y}$ the passive output as follows

$$\dot{\mathcal{V}}(\tilde{x}) \leq \tilde{y}^T \tilde{u}, \tag{14}$$

where $\tilde{y}_i = \tilde{x}^T \mathcal{J}_i x^\star$.

Note that Expression (14) can help us to design a stable controller if and only if the set of control inputs $\tilde{u}$ is selected such that this expression is always negative semidefinite. These characteristics are presented in the next section using a PI controller.

3.3. PI-PBC Design

To obtain a general control law to guarantee closed-loop stability in the sense of Lyapunov, let us employ the following PI control structure

$$\tilde{u} = -\mathcal{K}_p \tilde{y} + \mathcal{K}_i z, \tag{15a}$$

$$\dot{z} = -\tilde{y}, \tag{15b}$$

where $\mathcal{K}_p \succ 0$ and $\mathcal{K}_i \succ 0$ are the proportional and integral gain matrices and z is an auxiliary vector of variables related to the integral action.

To prove stability with the control law defined by Equation (15), let us modify the candidate Lyapunov function in Equation (12) as follows

$$\mathcal{W}(\tilde{x}, z) = \mathcal{V}(\tilde{x}) + \frac{1}{2} (z - z_o)^T \mathcal{K}_i (z - z_o), \tag{16}$$

with $z_o = \mathcal{K}_i^{-1} u^\star$ and its derivative is

$$\dot{\mathcal{W}}(\tilde{x}, \tilde{y}) = -\tilde{x}^T \mathcal{R} \tilde{x} - \tilde{y}^T \mathcal{K}_p \tilde{y} \leq 0, \tag{17}$$

which proves that the control input in Equation (15) guarantees stability in the sense of Lyapunov for closed-loop operation. Observe that in Equation (16), we consider that $\mathcal{K}_i = \mathcal{K}_i^T$.

Remark 4. *The control input Equation (15) can guarantee asymptotic stability in the sense of Lyapunov as proved in [15] by referring to Barbalat's lemma [14].*

4. Control Structure and Physical Constraint

This section presents the mathematical structure of the control laws for active and reactive power support with SCES systems, as well as the physical constraint that imposes the interconnection of a supercapacitor for energy storage applications.

4.1. Control Law

The presented PI-PBC approach can deal with parametric uncertainties in the SCES system when it is modeled using a direct power formulation (see Model (7) and (8)). For its analysis, let us present the general control inputs obtained from Equation (15) as follows

$$u_d = u_d^\star + k_{p1} \left(v^\star \left(p - p^\star \right) - p^\star \left(v - v^\star \right) \right) + k_{i1} \int \left(v^\star \left(p - p^\star \right) - p^\star \left(v - v^\star \right) \right) dt, \tag{18a}$$

$$u_q = u_q^\star + k_{p2} \left(q^\star \left(v - v^\star \right) - v^\star \left(q - q^\star \right) \right) + k_{i2} \int \left(q^\star \left(v - v^\star \right) - v^\star \left(q - q^\star \right) \right) dt, \tag{18b}$$

where k_{p1} and k_{p2} are the proportional gains, and k_{i1} and k_{i2} are the integral gains, respectively.

Remark 5. *The components $u_d^\star$ and $u_q^\star$ in Equation (18) can be neglected as recommended in [16] because they can be considered as constant values to calculate integral actions.*

It is important to mention that the control inputs of Equation (18) can remain robust to parametric uncertainties because they do not depend on any parameter of the system. This implies that small variations in these values (e.g., l, r, and c_{sc}) will not compromise the dynamical performance of the SCES system.

Note that in Equation (18), the value of $v^\star = v_d v_{sc}^\star$ needs to control the active and reactive power interchange between the SCES system and the grid (the values of $p^\star$ and $q^\star$ are defined by the designer because the main interest in SCES applications corresponds to control active and reactive power independently). Therefore, it is necessary to know $v_{sc}^\star$ to apply the controller. We start from the energy function of the SCES to compute $v_{sc}^\star$, as follows:

$$W_{sc}^\star = \frac{1}{2} C_{sc} v_{sc}^{\star\,2} \rightarrow \dot{W}_{sc}^\star = p_{sc}^\star = C_{sc} \dot{v}_{sc}^{\star\,2}, \tag{19}$$

and the relation between the active power of SCES and VSC can be approximated to $p_{sc}^\star = -p^\star$. Hence, $v_{sc}^\star$ can be given by

$$v_{sc}^{\star\,2} = \frac{1}{C_{sc}} \int -p^\star dt \rightarrow v_{sc}^\star = K_i \sqrt{\int_0^t -p^\star dt}, \tag{20}$$

with $K_i > 0$.

It is important to mention that the stability proof shown in Section 3.3 may be compromised by replacing Equation (20) into (18), which is only valid when $v_{sc}^\star$ is constant. Therefore, we adopted the time-scale separation assumption between the outer-loop ($v_{sc}^\star$) and the inner PI-PBC described in [17,18]. Interestingly, the assumption deals with the possible lost stability by only adjusting the integral gain in Equation (20).

4.2. Physical Operative Constraint

The energy storage capability of a SCES system is limited by the energy capabilities of the supercapacitor as well as for the admissible voltages in its terminals.

Figure 1 presents the dynamic behavior of the total energy stored in the SCES. In this figure, there are three critical points called O, P, and Q. Point O presents the minimum voltage value permissible in the supercapacitor terminals ($v_{sc}^{\min}$) that produce the value of the admissible minimum energy stored

($E_{\min}$); this voltage value is the lower bound in the SCES operation to guarantee the controllability of the closed-loop system. Additionally, point Q is the upper bound of the energy storage variable, which reaches the maximum permissible energy stored in the supercapacitor device ($v_{sc}^{\max} \leftrightarrow E_{\max}$), whereas point P represents some operating points between extreme points of O and Q.
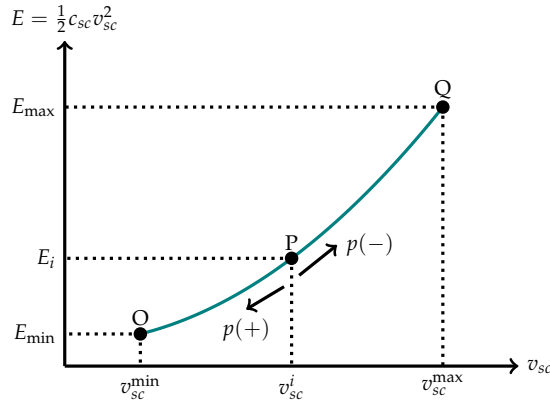

Figure 1. Behavior of the energy stored in the Supercapacitor energy storage (SCES).

Observe that point P allows positive or negative active power references. In the case in which p is positive, the energy stored decreases from point P to point O. In the case in which p is negative, the energy stored increases from point P to point Q. When point P is at the extreme points, we can conclude that if it is at point O, the reference for p can only be negative or zero, and if it is at point Q, it must be positive or zero. These are necessary conditions to preserve the useful life in the SCES.

5. Test System and Simulation Scenarios

5.1. The System Under Study

A low-voltage microgrid is used to test the DPC model of the SCES system. The test system is depicted in Figure 2, which contains two SCES systems. Additionally, it has a wind power generator and unbalanced loads to generate power oscillations in the system, thus allowing SCES to compensate for oscillations. The test system data can be consulted in [2].

To assess the capability and robustness of the proposed controller, the controller is compared with interconnection and damping assignment IDA-PBC presented in [19]. The IDA-PBC was performed under the $\alpha\beta$ reference frame. This implies that a PLL does not need to be implemented. However, it requires the derivatives of the desired values and the parameters of the system to be employed. This entails that the implementation of the IDA-PBC is more complicated than the proposed controller.

5.2. Simulation Scenarios

The SCES system can be used in various forms as support of active and reactive power oscillations in distributed generation applications with the wind turbine generator or can compensate for power oscillations provided by unbalanced loads [19]. According to this, in this study, two scenarios are designed to assess the performance and robustness of the SCES system using the DPC model and the proposed controller. The scenarios are as follows:

- **Scenario 1 (S1)**: Check the proposed controller to manage the active and reactive power independently in the SCES system.
- **Scenario 2 (S2)**: Evaluate the performance of the proposed controller applied to the SUCCESS system using the DPC model to relieve the oscillations of active and reactive power in the microgrid. This scenario employs a wind power generator located at bus 2, which provides active power and absorbs the reactive power shown in Figure 3. Additionally, the test system has two

demands (see DL1 and DL2 loads in Figure 2), which draw active and reactive power, as depicted in Figure 4.
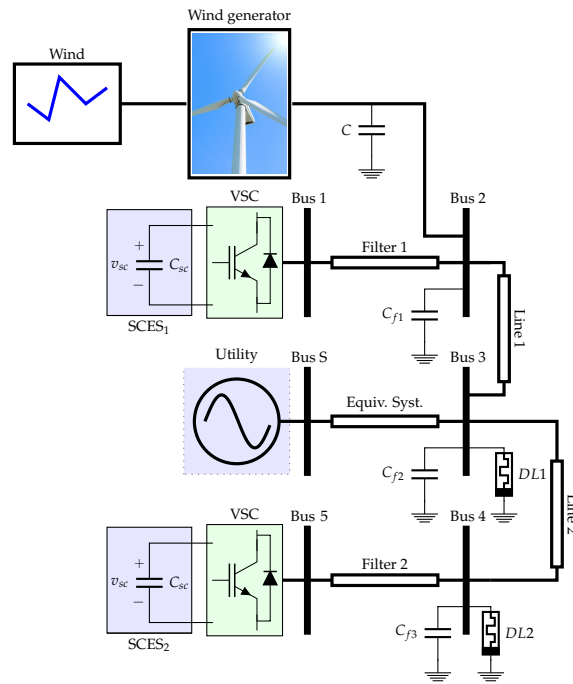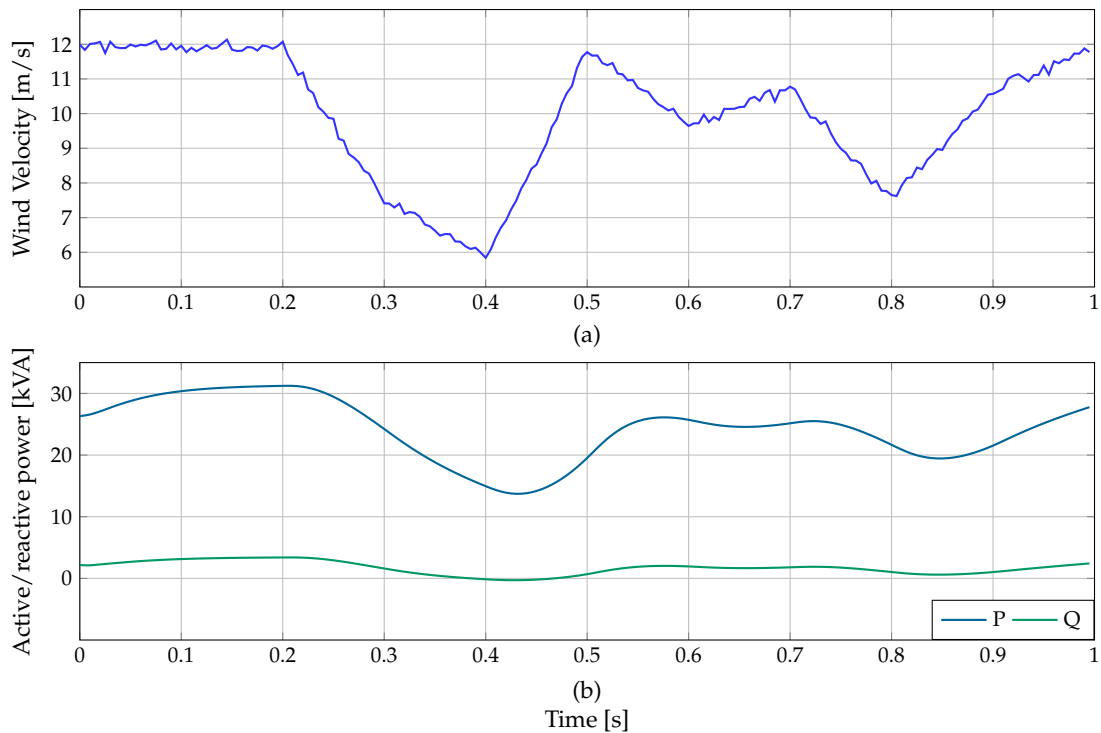

Figure 2. Test system configuration.

Figure 3. Wind generator: (**a**) wind profile and (**b**) active power provided and reactive power absorbed.
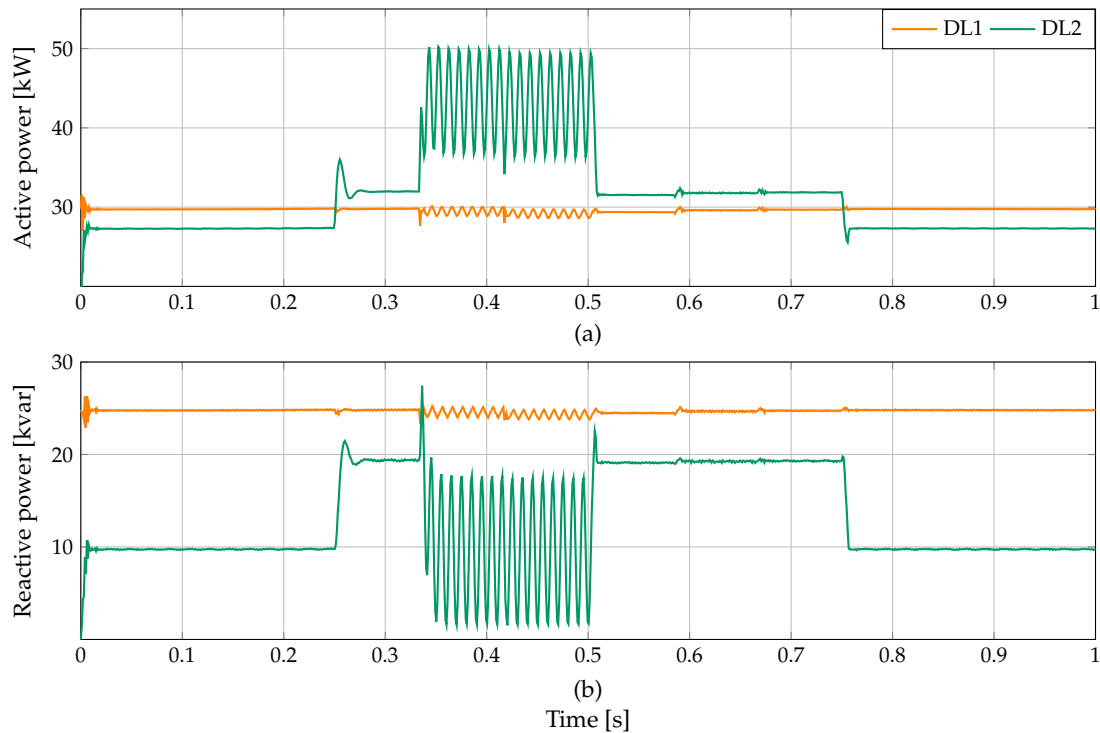
Figure 4. DL1 and DL2 loads: (**a**) active power demanded and (**b**) reactive power demanded.

It is important to mention that these scenarios have been designed arbitrarily to validate the accuracy and robustness of the DPC model and the proposed controller.

6. Results

The test system (see Figure 2) was implemented in MATLAB/Simulink and was executed on a desk-computer INTEL(R) Core(TM) i7–7700 CPU, 3.60 GHz, 8 GB RAM with 64-bits Windows 10 Professional by using MATLAB2019b. The switching frequency for the VSCs was fixed at 5 kHz. The parameters for the PI-PBC approach were tuned using the diagonal method developed in [20], which is suitable when the connection between the internal control of the model and the PI controller is lost, as presented with the proposed controller in this paper. The PI controller is computed, as follows:

$$k_{p_{12}} = \frac{\ln(9)L}{t_s}, k_{i_{12}} = \frac{\ln(9)R}{t_s}, \tag{21}$$

where L and R are values of the inductance and resistance of the AC filter and $t_s = 10^{-4}$ is the desired settling time.

6.1. Scenario 1

This scenario analyzes the performance of the PI-PBC to control the active and reactive power regardless of the SCES system applied to the DPC model. Here, we select arbitrary values for active and reactive power references to demonstrate the ability of the proposed controller. Figure 5 shows the dynamic behavior at the DC side of the SCES system and their active and reactive power outputs.
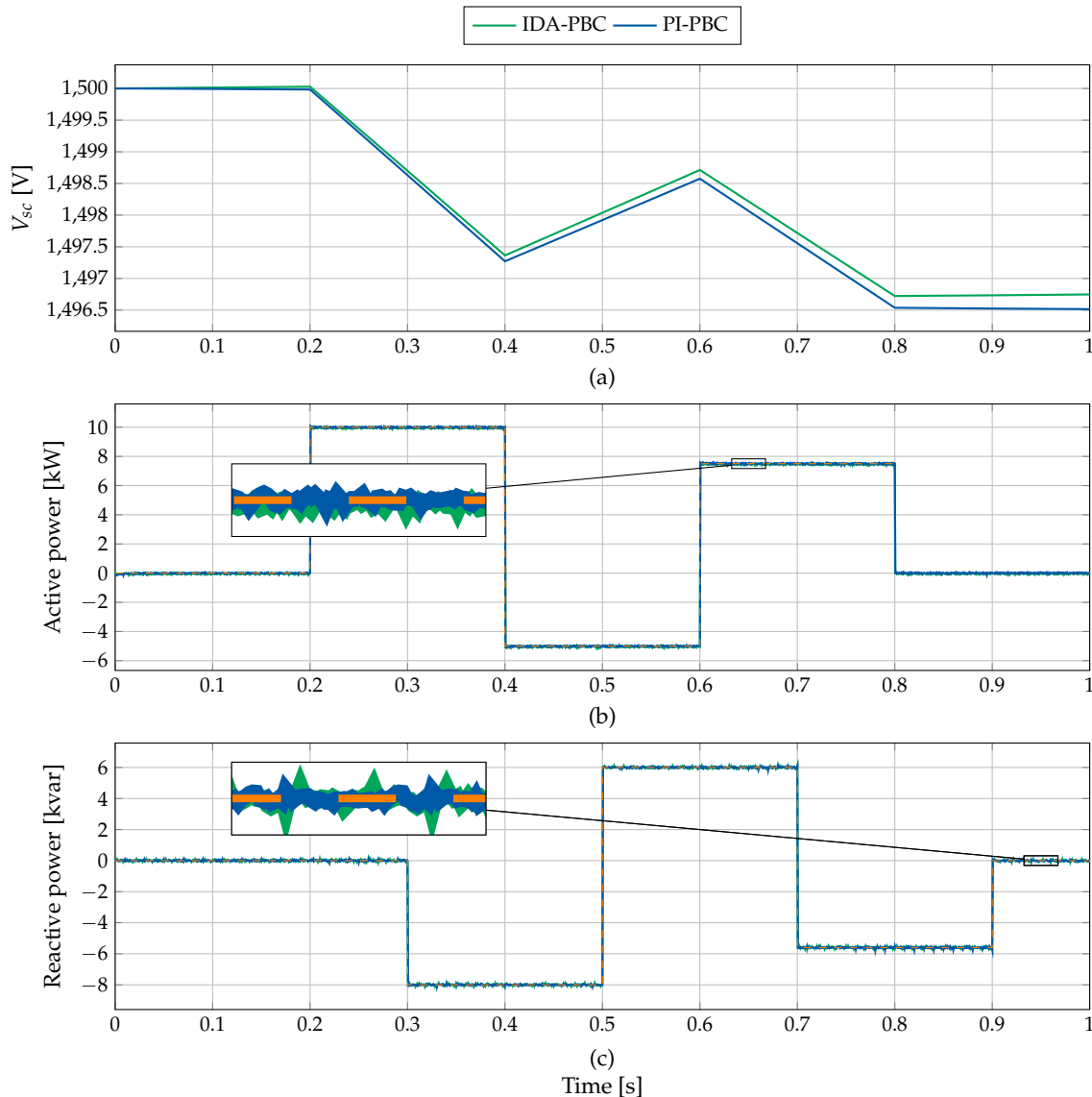
Figure 5. Dynamic behavior of the SCES system for S1: (**a**) supercapacitor voltage; (**b**) active power provided; and (**c**) reactive power absorbed.

Figure 5 shows that both controllers present a similar dynamic behavior. Nevertheless, PI–PBC presents a better performance compared with the IDA-PBC because it shows lower active and reactive power ripples. The ripples for the proposed controller are approximately 80 W and 85 var for the active and reactive power, respectively. In contrast, the ripples are about 100 W and 115 var when the IDA-PBC is implemented, respectively.

6.2. Scenario 2

This scenario investigates the ability of the SCES system using the DPC model to compensate for the power oscillations in the test system. Therefore, two SCES systems are considered, located at buses 1 and 5 (see Figure 2). The first SCES system relieves the power oscillation introduced by the wind power generator at bus 2. Here, we assume that the SCES system must keep active power at 28 kW and supply all the requirements of the reactive power of the generator. In contrast, the second SCES system compensates for the power oscillations provided by DL2 demands at bus 4, maintaining its active and reactive power at 30 kW and zero, respectively.

Figures 6 and 7 illustrate the dynamic behaviors at the DC side of the first and second SCES systems, respectively. In addition, their respective active and reactive powers are also plotted.
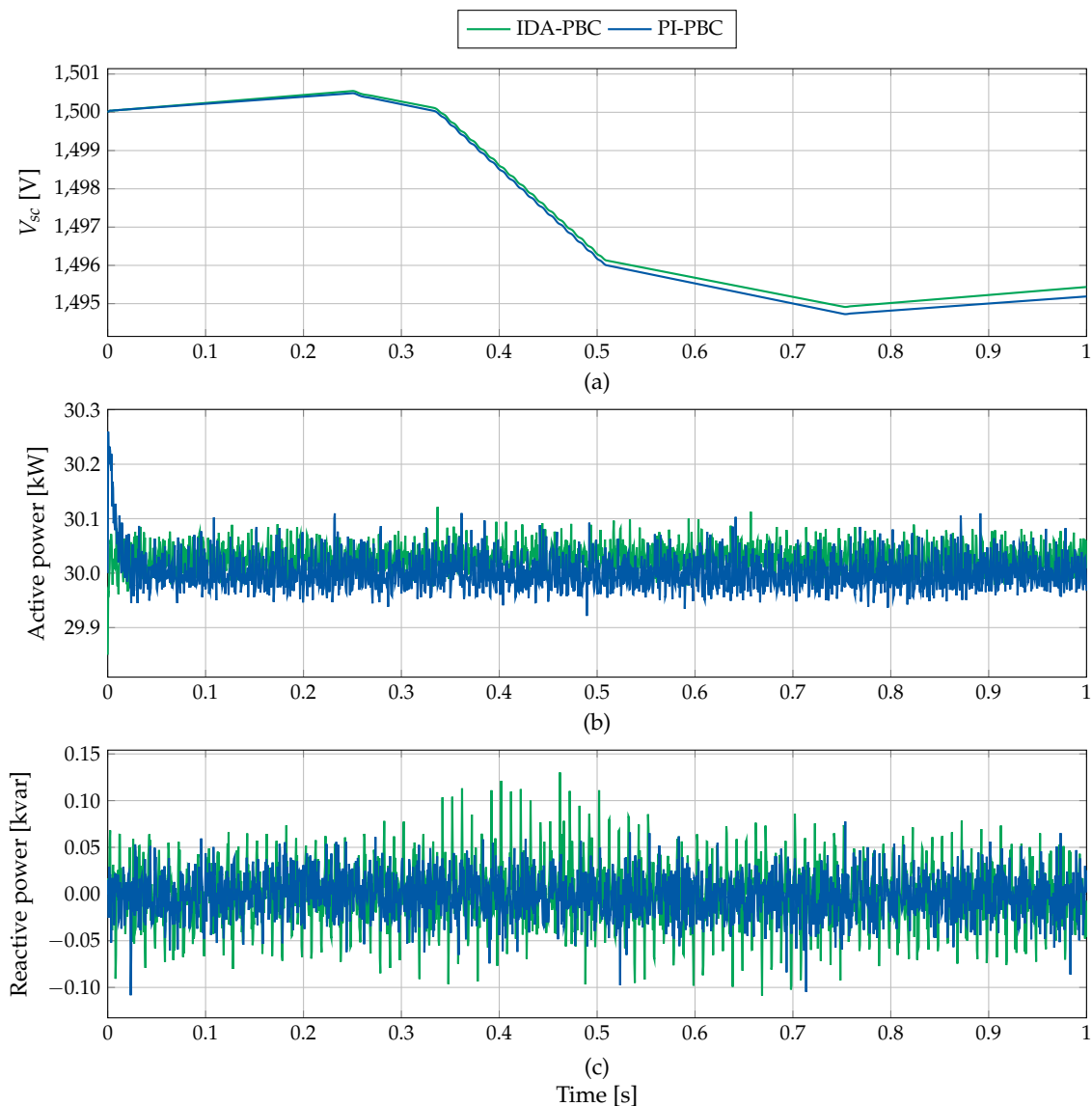

Figure 6. Dynamic behavior of the first SCES system for S2: (**a**) supercapacitor voltage; (**b**) active power provided; and (**c**) reactive power absorbed.

Observe in Figure 6 that both controllers maintain the control objectives ($p = 30$ kW and $q = 0$ kvar). However, the PI-PBC method continues presenting a better performance with lower ripples for the active and reactive power. Moreover, IDA-PBC has a steady-state error for active power of around 25 kW.

Note in Figure 7 that the proposed controller continues to show an enhanced response of active power, without steady-state error, as presented with the IDA-PBC. This behavior occurs because the IDA-PBC works as a proportional control. In contrast, the proposed controller includes an integral action that removes this error.
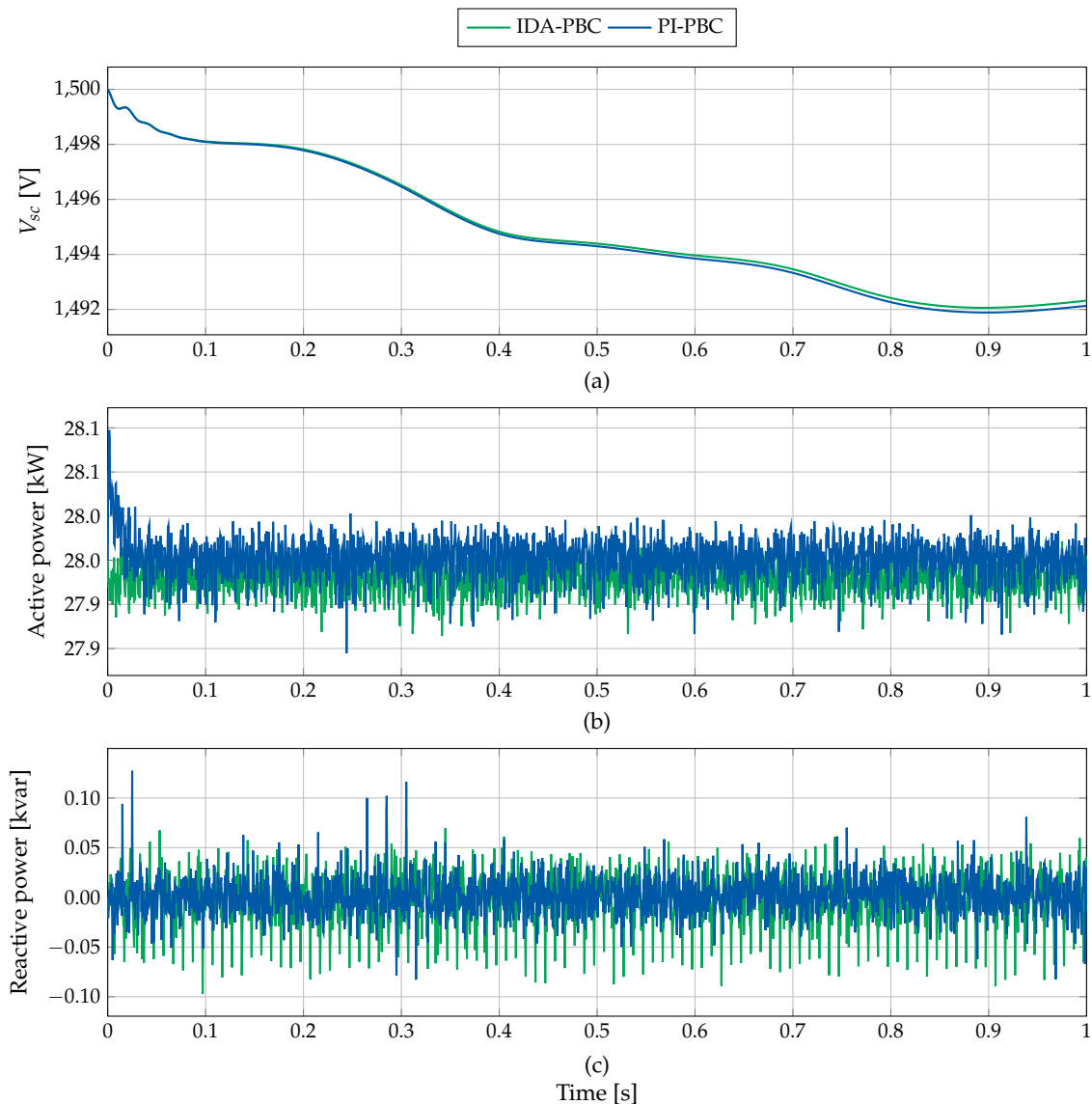
Figure 7. Dynamic behavior of the second SCES system for S2: (**a**) supercapacitor voltage; (**b**) active power provided; and (**c**) reactive power absorbed.

Complementary Analysis

Mean absolute error (MAE) and integral of time multiply absolute error (ITAE) (for the active and reactive power), and total harmonic distortion (THD) (for the AC currents) are used to quantify the performance of the controllers. Table 1 depicts these indexes for each scenario analyzed.

In Table 1, both controllers have a notable low MAE and ITAE. Nevertheless, the PI-PBC approach performs better for tracking power references than the IDA-PBC approach. This finding is supported by the reduction of MAE_p and MAE_q by 12.1% and 21.8% in the worst-case scenario (see first and the second column in Table 1), respectively. While ITAE_p and ITAE_q were reduced by 16.9% and 21.25% in the worst-case scenario, respectively.

Table 1. Performance Indexes.

	MAE$_p$ [W]	MAE$_q$ [var]	ITAE$_p$	ITAE$_q$	THD [%]
Scenario 1					
IDA-PBC	43.39	30.93	10.69	7.72	1.57
PI-PBC	23.71	20.65	5.94	5.35	1.55
Scenario 2 with SCES$_1$					
IDA-PBC	28.26	23.79	7.01	5.98	0.99
PI-PBC	24.68	18.59	5.82	4.64	0.98
Scenario 2 with SCES$_2$					
IDA-PBC	21.39	18.76	5.28	4.66	1.82
PI-PBC	18.38	14.60	4.36	3.63	1.80

In Table 1, it can be observed that both controllers meet the THD limits for power electronic converters established in Standard IEEE-1547 [21] even though the proposed controller has lower THD than the IDA-PBC approach. This entails that the PI-PBC approach presents better wave quality and lower losses.

The robustness of the proposed controller is investigated by applying a sensitive analysis for filter parameters. We assume that there are RL-filter mismatches with a variation of $\pm50\%$ and $\pm40\%$ for R and L parameters, respectively, when active power must be kept in 10 kW. For this test, we generate 100 random mismatches with uniform distribution. Figure 8 depicts the error mean value of the active power ΔP_{mean} against plant-model mismatches. Observe in this figure, that the IDA-PBC approach has a greater variation for ΔP_{mean} than the PI-PBC approach. This demonstrates that the proposed controller presents a better performance when there is a plant-model mismatch. In Figure 8, it can also be noted that the resistance variations do not influence over the controllers performance, while inductance variations do affect the performance of the controllers. This effect tends to be linear and is greater when the IDA-PBC approach is implemented.
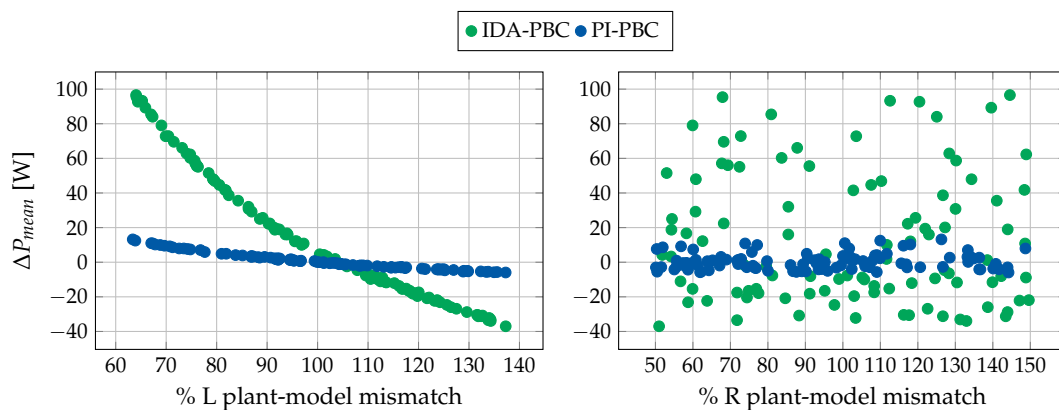
Figure 8. Sensitive analysis.

Remark 6. *The proposed controller does not show a remarkable difference in performance according to the IDA-PBC approach, which is easy to implement. This is because it only needs proportional-integral action and does not depend on the system parameters, while the IDA-PBC approach requires the system parameters and derivative calculation from the references to be applied.*

7. Conclusions

A direct power model developed from Park's reference frame for the SCES systems has been presented in this study. The direct power model controls instantaneous active and reactive powers regardless of the SCES system without employing typical phase-Locked-Loop. A PI-PBC approach was used to control the SCES system because it takes advantage of the pH structure of the SCES system to propose a control law that guarantees the stability of the system and exploits proportional-integral actions. The proposed controller demonstrates better performance in relieving the active and reactive power oscillations generated by wind generation considering imbalance when compared to the IDA-PBC approach.

Author Contributions: Conceptualization and writing—review and editing, W.G.-G. and O.D.M.; and supervision, writing—review and editing, F.M.S., C.A.R. and C.O.-H. All authors have read and agreed to the published version of the manuscript.

References

1. Mensah-Darkwa, K.; Zequine, C.; Kahol, P.K.; Gupta, R.K. Supercapacitor energy storage device using biowastes: A sustainable approach to green energy. *Sustainability* **2019**, *11*, 414. [CrossRef]
2. Gil, W.; Montoya, O.D.; Garces, A. Direct power control of electrical energy storage systems: A passivity-based PI approach. *Electr. Power Syst. Res.* **2019**, *175*, 105885.
3. Montoya, O.D.; Garces, A.; Espinosa-Perez, G. A generalized passivity-based control approach for power compensation in distribution systems using electrical energy storage systems. *J. Energy Storage* **2018**, *16*, 259–268. [CrossRef]
4. Aly, M.M.; Abdel-Akher, M.; Said, S.M.; Senjyu, T. A developed control strategy for mitigating wind power generation transients using superconducting magnetic energy storage with reactive power support. *Int. J. Electr. Power Energy Syst.* **2016**, *83*, 485–494. [CrossRef]
5. Montoya, O.D.; Gil-González, W.; Garces, A. SCES Integration in Power Grids: A PBC Approach under abc, $\alpha\beta0$ and dq0 Reference Frames. In Proceedings of the 2018 IEEE PES Transmission & Distribution Conference and Exhibition-Latin America (T&D-LA), Lima, Peru, 18–21 September 2018; pp. 1–5.
6. Haihua, Z.; Khambadkone, A.M. Hybrid modulation for dual active bridge bi-directional converter with extended power range for ultracapacitor application. In Proceedings of the 2008 IEEE Industry Applications Society Annual Meeting, Edmonton, AB, Canada, 5–9 October 2008; pp. 1–8.
7. Gil-González, W.J.; Garcés, A.; Escobar, A. A generalized model and control for supermagnetic and supercapacitor energy storage. *Ing. Cienc.* **2017**, *13*, 147–171. [CrossRef]
8. Thounthong, P.; Luksanasakul, A.; Koseeyaporn, P.; Davat, B. Intelligent model-based control of a standalone photovoltaic/fuel cell power plant with supercapacitor energy storage. *IEEE Trans. Sustain. Energy* **2012**, *4*, 240–249. [CrossRef]
9. Mufti, M.D.; Iqbal, S.J.; Lone, S.A.; Ain, Q. Supervisory Adaptive Predictive Control Scheme for Supercapacitor Energy Storage System. *IEEE Syst. J.* **2015**, *9*, 1020–1030. [CrossRef]
10. Montoya, O.D.; Gil-González, W.; Garces, A. Distributed energy resources integration in single-phase microgrids: An application of IDA-PBC and PI-PBC approaches. *Int. J. Electr. Power Energy Syst.* **2019**, *112*, 221–231. [CrossRef]
11. Montoya, O.D.; Gil-González, W.; Avila-Becerril, S.; Garces, A.; Espinosa-Pérez, G. Distributed Energy Resources Integration in AC Grids: A Family of Passivity-Based Controll, (in Spanish). *Rev. Iberoam. Autom. Inform. Ind.* **2019**, *16*, 212–221. [CrossRef]
12. Ortega, R.; Perez, J.A.L.; Nicklasson, P.J.; Sira-Ramirez, H.J. *Passivity-Based Control of Euler-Lagrange Systems: Mechanical, Electrical and Electromechanical Applications*; Springer Science & Business Media: Berlin/Heidelberg, Germany, 2013.

13. van der Schaft, A. *L2-Gain and Passivity Techniques in Nonlinear Control*; Springer: Berlin/Heidelberg, Germany, 2017.

14. Cisneros, R.; Pirro, M.; Bergna, G.; Ortega, R.; Ippoliti, G.; Molinas, M. Global tracking passivity-based PI control of bilinear systems: Application to the interleaved boost and modular multilevel converters. *Control Eng. Pract.* **2015**, *43*, 109–119. [CrossRef]

15. Zonetti, D. Energy-Based Modelling and Control of Electric Power Systems with Guaranteed Stability Properties. Ph.D. Thesis, Université Paris-Saclay, Saint-Aubin, France, 2016.

16. Zonetti, D.; Ortega, R.; Benchaib, A. A globally asymptotically stable decentralized PI controller for multi-terminal high-voltage DC transmission systems. In Proceedings of the 2014 European control conference (ECC), Strasbourg, France, 24–27 June 2014; pp. 1397–1403.

17. Zonetti, D.; Ortega, R.; Benchaib, A. Modeling and control of HVDC transmission systems from theory to practice and back. *Control. Eng. Pract.* **2015**, *45*, 133–146. [CrossRef]

18. Gil-González, W.; Montoya, O.D.; Garces, A. Direct power control for VSC-HVDC systems: An application of the global tracking passivity-based PI approach. *Int. J. Electr. Power Energy Syst.* **2019**, *110*, 588–597. [CrossRef]

19. Montoya, O.D.; Gil-González, W.; Serra, F.M. PBC Approach for SMES Devices in Electric Distribution Networks. *IEEE Trans. Circuits Syst. II Exp. Briefs* **2018**, *65*, 2003–2007. [CrossRef]

20. Harnefors, L.; Nee, H.P. Model-based current control of AC machines using the internal model control method. *IEEE Trans. Ind. Appl.* **1998**, *34*, 133–141. [CrossRef]

21. IEEE Standard for Interconnecting Distributed Resources with Electric Power Systems—Amendment 1. In *IEEE Std 1547a-2014 (Amendment to IEEE Std 1547-2003)*; IEEE: Piscataway, NJ, USA, 2014; pp. 1–16. [CrossRef]